Radiation-Driven Flame Spread Over Thermally-Thick Fuels in Quiescent Microgravity Environments

Youngjin Son and Paul D. Ronney
Department of Aerospace and Mechanical Engineering
University of Southern California, Los Angeles, CA 90089

Address correspondence to:

Youngjin Son
Department of Aerospace and Mechanical Engineering
University of Southern California
Los Angeles, CA 90089-1453
TEL: 1-213-740-3893
FAX: 1-213-740-8071
yson@usc.edu

Word count

Text including references:	= 3449 words (counted by Microsoft Word 2001)
Equations: 6	= 126 words (counted as 21 words each)
Nomenclature: 20	= 140 words (counted as 7 words each line)
Figures: 8	= 1700 words (Figure 2 counted as 300 words)
Total:	**= 5415 words**

Colloquium topic area: 7. Microgravity combustion

Keywords: Microgravity-Experiments, Microgravity-non-premixed, flame-spread

Submitted to
Twenty-Ninth International Symposium on Combustion,
Sapporo, Japan, July 21 – July 26, 2002.

Radiation-Driven Flame Spread Over Thermally-Thick Fuels in Quiescent Microgravity Environments

Youngjin Son and Paul D. Ronney
Department of Aerospace and Mechanical Engineering
University of Southern California, Los Angeles, CA 90089

Abstract

Microgravity experiments on flame spread over thermally-thick fuels were conducted using foam fuels to obtain low density and thermal conductivity, and thus large spread rate (S_f) over thermally-thick fuels compared to dense fuels such as PMMA. This scheme enabled meaningful results to be obtained even in 2.2 second drop tower experiments. It was found that, in contrast conventional understanding; steady spread can occur over thick fuels in quiescent microgravity environments, especially when a radiatively active diluent gas such as CO_2 is employed. This is proposed to be due to radiative transfer from the flame to the fuel surface that can lead to steady spread even when conductive heat transfer from the flame to the fuel bed is negligible. Radiative effects are more significant at microgravity conditions because the flame thickness is larger and thus the volume of radiating combustion products is larger at microgravity. The effects of oxygen concentration and pressure are shown and the transition from thermally-thick to thermally-thin behavior with decreasing bed thickness is demonstrated. A simple semi-quantitative model of radiation-driven flame spread rates is consistent with experimental observations. Radiative flux measurements confirm the proposed effects of diluent type and gravity level. These results are particularly noteworthy considering that the International Space Station employs CO_2 fire extinguishers; our results suggest that helium may be a better extinguishing agent on both mass and mole bases at microgravity even though CO_2 is much better on a mole basis at earth gravity.

Introduction

It is well known [1, 2, 3, 4] that convection influences flame spread over solid fuel beds in numerous ways. Flame spread is typically classified as opposed-flow, where the direction of flame propagation is opposite convective flow past the flame front, or concurrent-flow, where convection and spread are co-directional. Downward flame spread at earth gravity (1g) is characterized by opposed flow since the upward buoyant flow is opposite the direction of flame spread. At quiescent microgravity (μg) conditions, flame spread is necessarily opposed-flow (unless a forced flow is imposed) because the flame spreads toward the fresh atmosphere with self-induced convection velocity equal to the spread rate (S_f). At 1g, self-induced convection can justifiably be ignored since buoyancy-induced flows are typically 30 cm/sec, which is much higher than S_f, however, at μg self-induced convection is dominant.

As described by Williams [2], the basic approach to modeling S_f is to equate the heat flux per unit area from the gas to the fuel surface (q) to the rate of increase of solid fuel bed enthalpy, leading to

$$S_f = \frac{q\delta_g}{\rho_s C_{p,s}(T_v - T_\infty)\tau_s} \qquad (1),$$

where δ_g is the length of the zone over which heat is transferred from the gas to the fuel surface; for opposed-flow flame spread δ_g is proportional to the convection-diffusion zone thickness α_g/U where $\alpha_g \equiv \lambda_g/\rho_g C_{p,g}$, and U is the opposed flow velocity. If self-induced convection is included then $\delta_g = \alpha_g/(U+S_f)$.

For thermally-thin fuel beds (where transverse conduction within the fuel bed is negligible), heat transfer is via gas-phase conduction, thus $q \approx \lambda_g(T_f - T_v)/\delta_g$, where T_f is the flame temperature [1], thus

$$S_f = A\frac{\lambda_g}{\rho_s C_{p,s}\tau_s}\frac{T_f - T_v}{T_v - T_\infty} \qquad \text{(A = constant)} \qquad (2).$$

deRis [1] derived an approximate solution A=√2 and Delichatsios [5] found an "exact" solution A=π/4. For thermally-thin fuels steady spread is possible even at μg because, as Eq. 2 shows, this ideal S_f is independent of U.

For thermally-thin fuels, τ_s is the fuel bed half-thickness, whereas for thermally-thick (effectively semi-infinite) fuels, where heat conduction through the solid fuel is important, τ_s is the thermal penetration depth into the solid fuel (τ_p), estimated by equating q to the heat flux within the solid fuel=$\lambda_s[(T_v-T_\infty)/\tau_p]$:

$$\tau_p = \frac{\lambda_s (T_v - T_\infty)}{q} \Rightarrow S_f = \frac{q^2 \delta_g}{\rho_s C_{P,s} \lambda_s (T_v - T_\infty)^2} \tag{3}.$$

This result is identical to that derived by Tarifa and Torralbo [6] and deRis [1] for prescribed externally-imposed radiative sources, so the present approach is considered valid. If heat transfer to the fuel bed occurs via conduction, $q \approx \lambda_g (T_f - T_v)/\delta_g$ as for thin fuels, then the "exact" solution for S_f over thick fuels [1] is obtained (neglecting self-induced convection):

$$\tau_s = \frac{\lambda_{sy} \delta_g (T_v - T_\infty)}{\lambda_g (T_f - T_v)} \Rightarrow S_f = U \frac{\lambda_g \rho_g C_{p,g}}{\lambda_s \rho_s C_{p,s}} \left(\frac{T_f - T}{T_v - T_\infty} \right)^2 \tag{4}.$$

The transition from thermally-thin to thermally-thick behavior occurs when $\tau_s \approx \tau_p$. A given material may behave as thermally-thin or thermally-thick depending on δ_g and thus U.

Equation 4 shows that for thermally-thick fuels, $S_f \sim U$, suggesting that at μg, where U=0, no steady spread is possible. If self-induced convection ($U=S_f$) is considered then S_f is indeterminate unless forced flow is applied to generate some U independent of S_f. An unsteady heat conduction analysis for quiescent thermally-thick flame spread at μg [7] predicts that $\tau_s \sim (\alpha_s t)^{1/2}$ which results in $S_f \sim t^{-1/2}$, where t is the time lapse from ignition. The prevailing opinion [7] is that S_f should decrease continually until extinction occurs via radiative losses. Computations and space experiments [7, 8] supported these assertions.

In this work we show that this inability to obtain steady spread over thermally-thick fuels in quiescent μg environments no longer applies when heat transfer to the fuel bed via flame-generated radiation (in addition to or instead of conduction) is significant. Altenkirch and

collaborators [7, 8] considered flame radiation only as a loss mechanism. We derive an approximate expression for S_f and conduct μg experiments that demonstrate the proposed mechanism of flame spread with flame-generated radiation.

As evidence of the importance of this flame radiation, thin-fuel flame spread experiments [9] in radiatively-inert N_2, He or Ar diluents showed the conventional behavior where S_f is lower and the minimum flammable O_2 concentration is higher at μg. This occurs because when U is lower, δ is larger and the volume of radiating gases is higher. In contrast, for radiatively-active CO_2 and SF_6 diluents, the opposite behavior was observed where S_f is higher at μg. This was attributed to (1) increased radiative emission from CO_2 or SF_6, which increases the net heat flux to the fuel bed and (2) reabsorption of this radiation, which reduces radiative heat loss. (Diluent type also affects Lewis numbers but these effects were shown to be less important.)

Approximate analysis

When radiative heat transfer to the fuel bed is significant, S_f given by Eqs. 1 and 3 is still valid but Eq. 4 must be modified. For flame-generated radiation, q_r is coupled to the spread process itself. As a first estimate we consider optically-thin radiation, where no reabsorption occurs and spectral properties are grouped into one parameter. We assume the flame front to be an isothermal volume of optically-thin radiating gas at temperature T_f with dimension δ_g in both the directions parallel and perpendicular to the fuel bed. We make this choice because for optically-thin radiation no length scale exists, thus the thermal thickness of the flame is still determined by the convective-diffusive zone thickness δ_g. Of course, radiation can be transferred to the fuel bed from distances greater than δ_g, but this radiation is at small angles to the fuel surface and thus is not an effective heat transfer mechanism. The heat flux due to radiation can be estimated as $\Lambda\delta_g$, where $\Lambda=4\sigma a_P(T_f^4-T_v^4)$ is the radiation power per unit volume. The combined effects of gas-phase radiation and thermal conduction is then $q=\Lambda\delta_g+\lambda_g(T_f - T_v)/\delta_g$. Combining this with $\delta_g=\alpha_g/S_f$ and Eq. 4 leads to, assuming unit fuel bed emissivity and no forced convection (U=0),

$$S_f = \left[\frac{\Lambda \alpha_g^2}{\sqrt{\alpha_g \rho_s C_{P,s} \lambda_s (T_v - T_\infty)} - \lambda_g (T_f - T_v)} \right]^{1/2} \qquad (5).$$

Equation 5 predicts that without gas-phase radiation, no steady spread is possible (S_f=0) and with gas-phase radiation, $S_f \sim \Lambda^{1/2}$. Thus, increasing gas-phase radiation should increase S_f. Of course this also increases radiative loss, but the ratio of heat loss to heat generation will remain roughly constant. Equation 5 also shows that pressure effects are important since $\Lambda \sim P$ and $\alpha_g \sim P^{-1}$.

Radiative transfer to the fuel bed will also increase T_f [1], though using representative values of the thermodynamic and transport properties the predicted effect is too weak to affect the above conclusions. It does, however, increase the impact of radiative transport slightly stronger than that shown here.

Experimental apparatus

To test for the possibility of steady flame spread over thermally-thick fuels in quiescent μg environments, experiments were conducted in the NASA-Glenn 2.2 second drop tower and downward propagating (opposed-flow) comparison tests were performed at 1g. Experiments were performed in our existing flame spread apparatus [9]. The 20 liter chamber was filled with the desired atmosphere by partial pressures. The fuel samples (described below) were typically 10 cm × 11.5 cm and are held between aluminum quenching plates to inhibit edge-burning effects. Unless otherwise noted samples were 10 mm thick, which we shall show is well into the thermally-thick limit. Both single-sided and two-sided burning was examined; unless otherwise noted all results shown were for single-sided burning. After allowing time for settling of convection, the fuel samples were ignited by an electrically-heated Kanthal wire imbedded in a nitrocellulose membrane glued onto the fuel surface. Ignition was controlled and radiometer data are collected by a microcomputer on the drop package. The flame spread process was imaged using CCD cameras whose signals are connected via fiber-optic cables to ground-based video recorders. One camera was positioned with its viewing axis perpendicular the fuel sample plane to images the flame front and thus spread rate. Another camera imaged laser shearing interferograms of the flames from a side view to determine flame shape and thickness.

Narrow-angle thermopile-type radiometers mounted 10 cm from the fuel bed were used to determine radiative emissions from the flames. The measured radiative fluxes represent only the

flux reaching the detector through the narrow-angle radiometer and thus are much smaller than the total emissive power from the flame. Three radiometers were used: (1) a front-side (burning side) radiometer viewing a hole in the fuel bed to measure only the outward gas-phase radiative loss, (2) another front-side radiometer viewing the fuel surface to measure both the outward gas-phase and surface radiative fluxes, thus total radiative loss, (3) a back-side radiometer viewing through the hole to measures the inward gas-phase radiative heat flux, thus the fuel bed heating due to gas-phase radiation. The difference between (2) and (1) can be interpreted as the surface contribution to the total radiative loss.

The standard fuel for fundamental thick-fuel flame spread experiments is polymethylmethacrylate (PMMA) which has the thick-fuel spread rate parameter $\lambda_s\rho_s C_{P,s}(T_v-T_\infty)^2 \approx 3.3\times10^{10}$ J^2/m^{4}s. This leads to $S_f \approx 0.006$ cm/sec in air at 1atm, which is too low to observe steady-state flame spread in short-duration drop-tower experiments. After evaluating numerous candidate materials, we chose open-cell polyphenolic foams that have values of $\lambda_s\rho_s C_{P,s}(T_v-T_\infty)^2$ 2 to 3 orders of magnitude smaller than PMMA because the foams have much lower thermal conductivity (λ_s) and density (ρ_s) than PMMA. Polyphenolic foams were chosen primarily because they have lower sooting tendency and negligible melting or dripping tendency compared to other foams such as polystyrene or polyurethane. Of course all foams contain trapped gas, however, the density of the foams employed is at least 20 times larger than the test atmospheres, thus the trapped gas contributes negligibly contribution to the overall stoichiometry. The permeability of the foam (typically 10^{-7} m^2) is small enough that flow through the porous media is negligible. Equation 4 also shows that high pressure (thus high ρ_s) favors high S_f and was employed here.

Experimental results

It was found that steady flame spread could be obtained even in the short-duration μg experiments with the foam fuels at high pressures. Figure 1 shows that, as was also seen in the thin-fuel tests [9], for CO_2-diluted atmospheres S_f could be higher at μg than 1g, especially at low O_2 concentrations, but for N_2-diluted atmospheres S_f was always higher at 1g than μg. At μg, S_f can actually be higher in CO_2 than N_2 at the same O_2 concentration even though CO_2 has a larger C_P and thus yields lower T_f than N_2 for the same O_2 concentration. Figure 1 also shows

that for CO_2 diluent the minimum O_2 concentration supporting combustion is substantially lower at μg than 1g, whereas for N_2 the minimum O_2 concentration is higher at μg. All of these results show that flames in CO_2-diluted atmospheres burn more robustly at μg than 1g whereas the opposite trend is found for N_2. We propose that this is due to three factors. First, Λ is larger for O_2-CO_2 atmospheres (since both the combustion products and ambient atmosphere contain radiant species, whereas for O_2-N_2 only the combustion products radiate) which increases the heat flux to the fuel bed and thus S_f (see Eq. 5). Second, without buoyant convection (U=0), the flame thickness $\delta_g=\alpha_g/(U+S_f)$ is much thicker at μg than at 1g, thus μg flames have more volume and can transfer more radiation to fuel bed. Interferometer images (not shown) confirm that flames are much thicker at μg. This effect is more important for lower O_2 concentrations (thus lower S_f) which explains why the difference between 1g and μg spread rates in O_2-CO_2 atmospheres is larger at lower O_2 concentrations. Third, O_2-CO_2 atmospheres can reabsorb and re-radiate emitted radiation whereas O_2-N_2 atmospheres cannot, thus substantial radiative heat losses that would otherwise occur at μg with thick flames in strongly radiating O_2-CO_2 atmospheres are at least partially suppressed.

Figure 2 (upper) shows pressure effects on S_f. Except at low pressures, for CO_2 diluent S_f is higher at 1g than μg, whereas for N_2 diluent only at very high pressures is S_f higher at μg. The reversal of CO_2 behavior at low pressures may occur because flame thickness is larger at low pressure since α_g is larger and because absorption coefficient a_P is smaller at lower pressure, thus at sufficiently low pressure radiative loss may dominate reabsorption and re-radiation effects. S_f increases with increasing pressure until a plateau of S_f is reached for both μg and 1g cases. This transition may be due to transition to nearly opaque radiative conditions ($a_P^{-1}<\delta_g$) since a_P is larger at higher pressure. Figure 2 (lower) shows predicted pressure effects on S_f (Eq. 5) for O_2-CO_2 atmospheres at μg. Two different assumed values of T_f are shown. All gas properties are evaluated at the average temperature $(T_f+T_\infty)/2$. The model provides reasonable S_f estimates except near the low-pressure extinction limit, where heat losses may dominate, and at high pressure where there may be a transition to nearly opaque conditions. (Neither of these effects is included in the simple model leading to Eq. 5).

Figure 3 shows the effects of fuel bed thickness on spread rate for a fixed atmosphere. S_f is independent of thickness for sufficiently thick fuel beds, demonstrating thermally-thick conditions. The thickness at the start of the transition is about 2 mm for the cases shown. For

thick samples S_f is nearly the same for 1-sided and 2-sided burning, again indicating thermally-thick flame spread. For the thinnest samples S_f for 1-sided spread is about half that of 2-sided spread, which is consistent with the simple thermal model for thin fuels (Eqs. 1 and 2). Note however the odd behavior that S_f actually decreases with decreasing thickness, which is contrary to thin-fuel theory without radiation (Eq. 2) and will never occur without radiation because at the transition from thermally-thin to thermally-thick behavior ($\tau_p=\tau_s$) the values of S_f are equal for thin (Eq. 2) and thick (Eq. 4) fuels. With radiative effects this is no longer true; S_f for thick fuels is given by Eq. 5 and for thin fuels is determined from Eq. 1 using $q=\Lambda\delta_g+\lambda_g(T_f - T_v)/\delta_g$ and $\delta_g=\alpha_g/(U+S_f)$, leading to a cubic equation for S_f:

$$\left(\frac{S_f}{S_{f,o}}\right)^3+\left(\frac{2U}{S_{f,o}}-1\right)\left(\frac{S_f}{S_{f,o}}\right)^2+\frac{U}{S_{f,o}}\left(\frac{U}{S_{f,o}}-2\right)\left(\frac{S_f}{S_{f,o}}\right)-\left(U^2+\left(\frac{S_{f,rad}}{S_{f,o}}\right)^3\right)=0 \qquad (6)$$

where $S_{f,o}$ is the radiation-free spread rate (Eq. 2) and $S_{f,rad}=[\Lambda\alpha_g^2/\rho_s C_{P,s}\tau_s(T_v-T_\infty)]^{1/3}$ is the without conduction to the fuel bed. (The effect of U for thick fuels can be computed in the same way, but the resulting fifth-order polynomial is too long to print here.) It can be shown that at the transition point $\tau_p=\tau_s$, the thin-fuel S_f (Eq. 6) can be lower than the thick-fuel S_f (Eq. 5), leading to non-monotonic effects of τ_s on S_f. Moreover, this behavior can occur with or without an imposed or buoyant flow U, thus the behavior can be seen at both 1g and μg. (The foams could not be sliced thin enough to observe conventional thin-fuel behavior at μg (S_f increasing as τ_s decreases) but this behavior is seen for 1g flame spread in Fig. 3.)

Figure 4 shows that, as expected, S_f decreases with increasing fuel bed density for both 1g and μg conditions.

Figures 5a-d show the radiative characteristics of O_2-CO_2 and O_2-N_2 flames at 1g and μg. The only case where the back-side radiometer (which measures the gas-phase radiant heat flux to the fuel bed; see Experimental Apparatus) shows comparable intensity and timing with the two front-side radiometers is for the radiatively active O_2-CO_2 atmosphere at μg (Fig. 6a). This is probably because only in this case is there substantial emission, absorption and re-emission, which is the only means to obtain substantial radiative flux to the back-side radiometer. O_2-N_2 atmospheres do not show this behavior at all, and even for O_2-CO_2 atmospheres this is seen only

at μg where δ_g is larger and thus the total radiative flux $\sim\Lambda\delta_g$ is greater. Note also that the gas-phase radiative loss ("Front, gas only" curves) at μg is actually lower for O_2-CO_2 than O_2-N_2 atmospheres due to reabsorption by the ambient atmosphere for O_2-CO_2. At 1g (Figs. 6b and 6d) the surface radiation (the difference between the two front-side radiometer readings) is much larger than gas-phase radiation due to the decreased flame thickness thus decreased volume of radiating gas at 1g. These results confirm our hypotheses concerning radiative transfer effects on μg flame spread, in particular that (1) radiative preheating of the fuel bed by the gas is significant in radiatively-active atmospheres at μg, (2) reabsorption effects can prevent massive heat losses (thus extinction) in radiatively-active atmospheres at μg and (3) these effects are less important at 1g due to substantial U caused by buoyancy which leads to smaller flame thicknesses thus less volume of radiating gas.

Discussion and conclusions

Microgravity experiments on flame spread over thermally-thick fuels were conducted using foam fuels to obtain low density and thermal conductivity, and thus large spread rate (S_f) compared to dense fuels such as PMMA. This scheme enabled meaningful results to be obtained even in 2.2 second drop tower experiments. It was found that, in contrast to conventional understanding, steady spread could occur over thick fuels in quiescent μg environments, especially when a radiatively active diluent gas such as CO_2 is employed. In some cases with CO_2 diluent the spread rate was actually higher at μg than at 1g despite the absence of convection at μg, which without radiative transfer is expected to preclude the possibility of steady spread. This was shown to be due to radiative transfer from the flame to the fuel surface. This assertion is consistent with measurements of the radiatively fluxes to and from the fuel bed. This conclusion was also supported by interferometer images showing that the flames where much thicker at μg than 1g, indicating that the μg flames have more volume and thus can radiate more heat to the fuel bed. Additionally, the transition from thermally-thick to thermally-thin behavior with decreasing bed thickness was demonstrated, at a typical fuel bed thickness of 2 mm.

These results are relevant to studies of fire safety in manned spacecraft, particularly the International Space Station that uses CO_2 fire extinguishers. CO_2 may not be as effective as an

extinguishing agent at μg as it is at 1g in some conditions because of the differences in spread mechanisms at 1g and μg. In particular, the difference between conduction-dominated heat transport to the fuel bed at 1g vs. radiation-dominated heat transport at μg indicates that radiatively-inert diluents such as helium could be preferable in μg applications.

With this motivation, several tests were conducted using He diluent at 4 atm. It was found that He- and CO_2-diluted atmospheres exhibit nearly the same S_f, for a given O_2 mole fraction even though CO_2 has a mole-based C_P at 300K that is 1.8 times higher than He, and at 2000K is 3.9 times higher. Also, He has a thermal conductivity (λ_g) 9.4 times higher than CO_2. Both of these factors should lead to higher T_f and S_f in He than in CO_2-diluted atmospheres at the same O_2 concentration (see Eqs. 3 and 5). Furthermore, at 1g the minimum O_2 mole fraction supporting combustion was nearly the same (30%) in He and CO_2-diluted atmospheres whereas at μg the minimum O_2 mole fraction was much higher for He (35%) than CO_2 (27%). There are at least three reasons for the observed behavior. First, the Lewis number of O_2 in He is much higher than O_2 in CO_2 (≈1.20 vs. ≈0.84), which leads to lower spread rates for He [10]. Second, the higher λ_g and α_g of He leads to thicker flames and thus greater radiative loss for the same S_f. Third, unlike CO_2, He is radiatively non-participating and thus no reabsorption or re-emission occurs. Consequently, we conclude that He may be a superior fire suppression agent at μg on several bases. First, at μg He is more effective than CO_2 on a mole basis (thus pressure times storage volume basis), meaning that the size and weight of storage bottles would be smaller for the same fire-fighting capability. Second, He is much more effective on a mass basis (by about 11x) at μg. Third, He has no physiological activity, unlike CO_2 which affects human respiration. Fourth, as compared to N_2 or CO_2, He is not very soluble in water and thus has less tendency to cause bloodstream bubble formation following rapid spacecraft cabin depressurization.

Nomenclature

a_P	Planck mean absorption coefficient
C_P	constant-pressure heat capacity
q_r	radiant heat flux per unit area
q_λ	radiant heat flux per unit wavelength
S_f	flame spread rate over solid fuel bed
T	temperature
U	convection velocity
α	thermal diffusivity

δ flame thickness
λ thermal conductivity
Λ radiative heat transfer per unit volume
ρ density
τ_s fuel bed half-thickness (thin fuel)
τ_p thermal penetration depth (thick fuel)
σ Stefan-Boltzman constant

Subscripts
f flame front condition
g gas-phase condition
s solid fuel or solid surface condition
v solid fuel vaporization condition
∞ ambient conditions

Acknowledgments

This work was supported by NASA-Glenn Research Center under grant NCC3-671. The authors are grateful to Dr. Suleyman Gokoglu, Dr. Linton Honda and the NASA-Glenn 2.2-second drop tower staff for many helpful discussions and technical support.

References

1. deRis, J.N., *Proc. Combust. Inst.* 12:241 (1969).

2. Williams, F.A., *Proc. Combust. Inst.* 12:1281 (1976).

3. Fernandez-Pello, A.C., *Combust. Flame* 30:119 (1984).

4. Wichman, I. S., *Prog. Energy Combust. Sci*. 18:553 (1992).

5. Delichatsios, M. A., *Combust. Sci. Tech*. 44:257 (1986).

6. Tarifa, C.S., Torralbo, A.M., *Proc. Combust. Inst.* 11:533-544 (1967).

7. Bhattacharjee, S., West, J., Altenkirch, R.A., *Proc. Combust. Inst.* 26:1477 (1996).

8. Altenkirch, R.A., Tang, L., Sacksteder, K., Bhattacharjee, S., Delichatsios, M.A., *Proc. Combust. Inst.* 27:2515 (1998).

9. Honda, L.K., Ronney, P.D., *Combust. Sci. Tech*. 133:267 (1998).

10. Zhang, Y., Ronney, P.D., Roegner, E., Greenberg, J.B., *Combust. Flame* 90:71 (1992).

Figure Captions

Figure 1. Effects of oxygen concentration on spread rates over thick solid fuel beds at μg and 1g, polyphenolic foam, density: 0.0267 g/cm^3, 4 atm total pressure.

Figure 2. Effects of pressure on spread rate over thick solid fuel beds at μg and 1g, polyphenolic foam, density: 0.0267 g/cm^3. Upper: 40%O_2-60%CO_2 and : 40%O_2-60%N_2, 1g and μg. Lower: 40%O_2-60%CO_2 at μg only, along with spread rate estimates based on Eq. 5 assumed flame temperatures of 1500K and 1800K. In these estimates, all gas properties are calculated using temperature averaging between ambient temperature and flame temperature.

Figure 3. Effects of fuel bed thickness on spread rate over solid fuel beds at μg and 1g, polyphenolic foam, density: 0.0267 g/cm^3, 40%O_2-60%CO_2, 4 atm total pressure.

Figure 4. Effect of fuel bed density on spread rate over thick solid fuels beds at μg and 1g, polyphenolic foam, 40%O_2-60%CO_2, 4 atm total pressure.

Figure 5. Radiative flux characteristics of flames spreading over thick polyphenolic foam fuel. See Experimental Apparatus section for discussion of the interpretation of radiometer data.

(a) 40%% O_2 - 60% CO_2, 4 atm, μg.
(b) 40%% O_2 - 60% CO_2, 4 atm, 1g.
(c) 40%% O_2 - 60% N_2, 4 atm, μg.
(d) 40%% O_2 - 60% N_2, 4 atm, 1g.

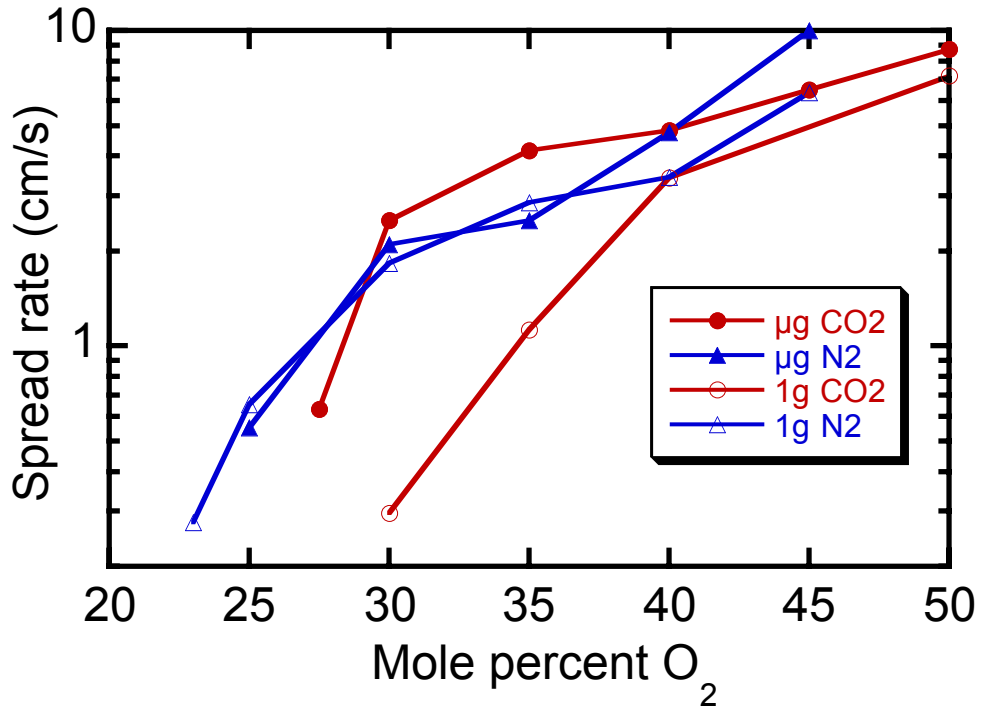

Figure 1. Effects of oxygen concentration on spread rates over thick solid fuel beds at µg and 1g, polyphenolic foam, density: 0.0267 g/cm^3, 4 atm total pressure.

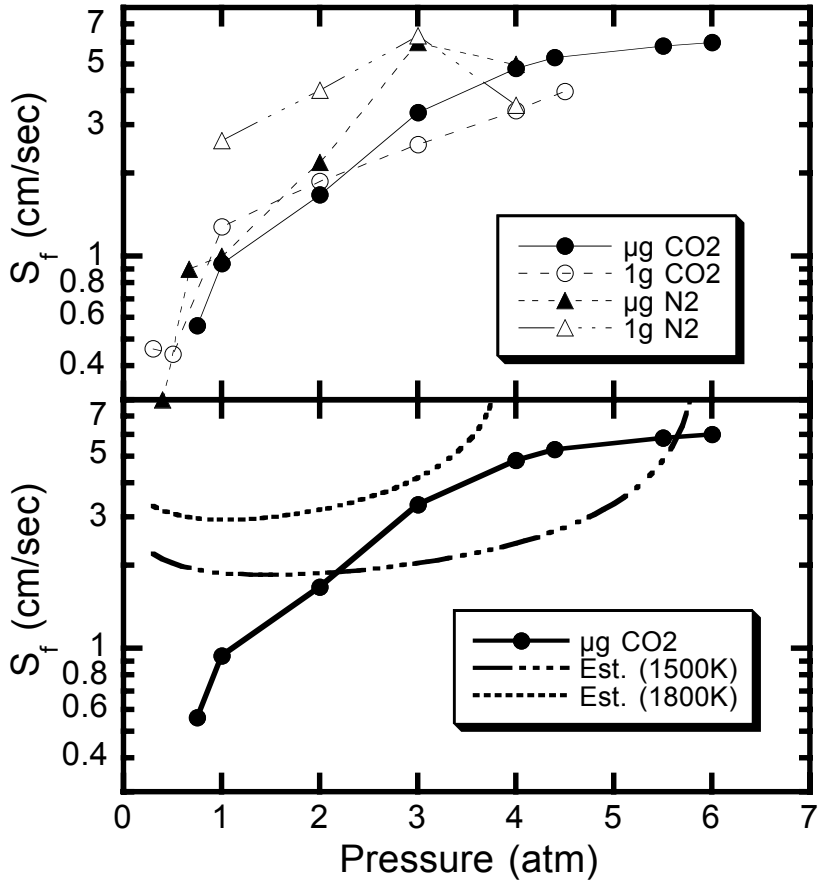

Figure 2. Effects of pressure on spread rate over thick solid fuel beds at μg and 1g, polyphenolic foam, density: 0.0267 g/cm^3. Upper: 40%O_2-60%CO_2 and : 40%O_2-60%N_2, 1g and μg. Lower: 40%O_2-60%CO_2 at μg only, along with spread rate estimates based on Eq. 5 assumed flame temperatures of 1500K and 1800K. In these estimates, all gas properties are calculated using temperature averaging between ambient temperature and flame temperature.

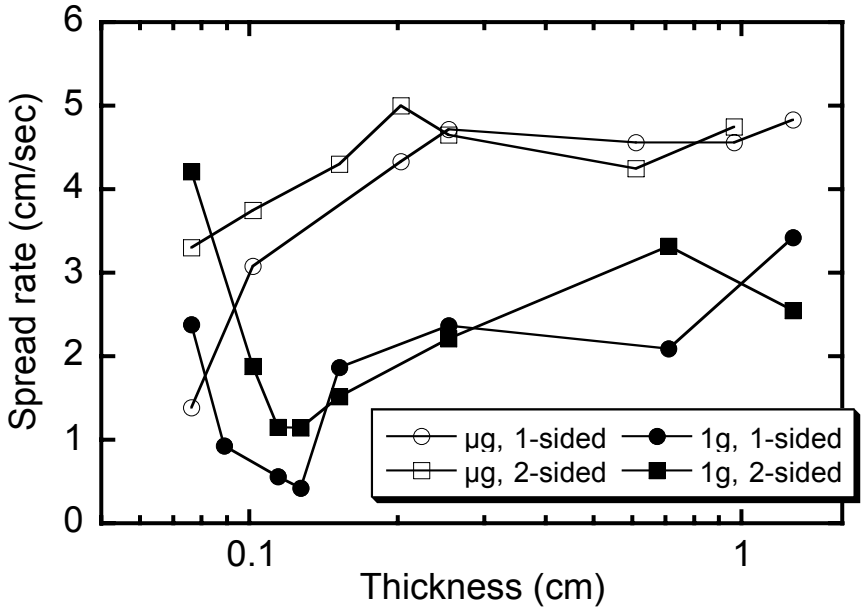

Figure 3. Effects of fuel bed thickness on spread rate over solid fuel beds at μg and 1g, polyphenolic foam, density: 0.0267 g/cm^3, 40%O_2-60%CO_2, 4 atm total pressure.

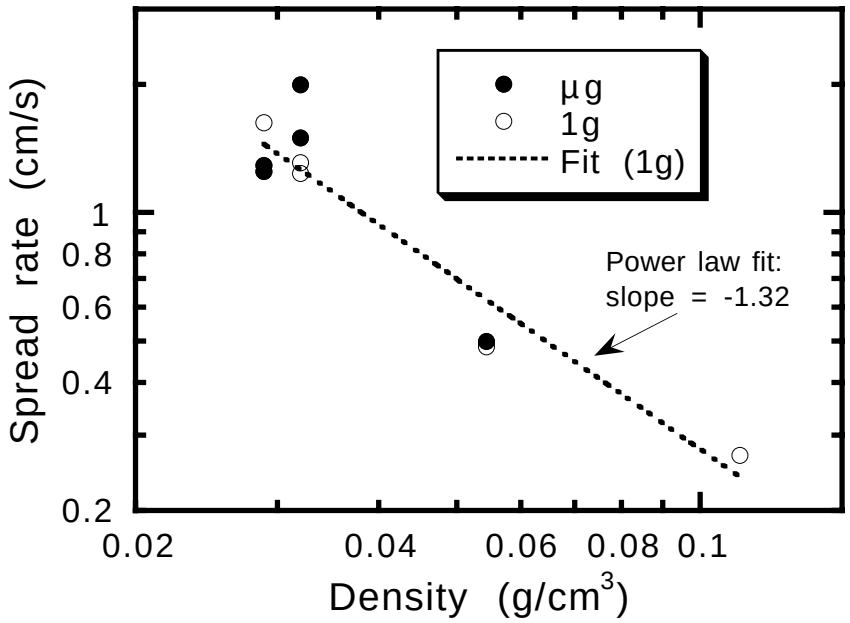

Figure 4. Effect of fuel bed density on spread rate over thick solid fuels beds at µg and 1g, polyphenolic foam, 40%O_2-60%CO_2, 4 atm total pressure.

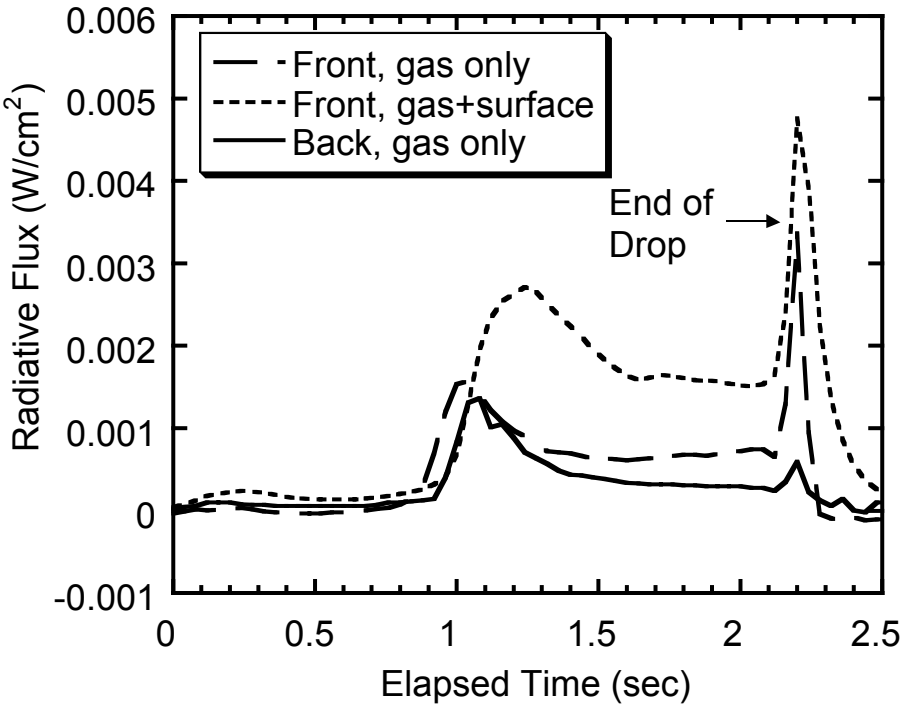

Figure 5. Radiative flux characteristics of flames spreading over polyphenolic foam fuel. See Experimental Apparatus section for discussion of the interpretation of radiometer data.
(a) 40%% O_2 - 60% CO_2, 4 atm, μg.

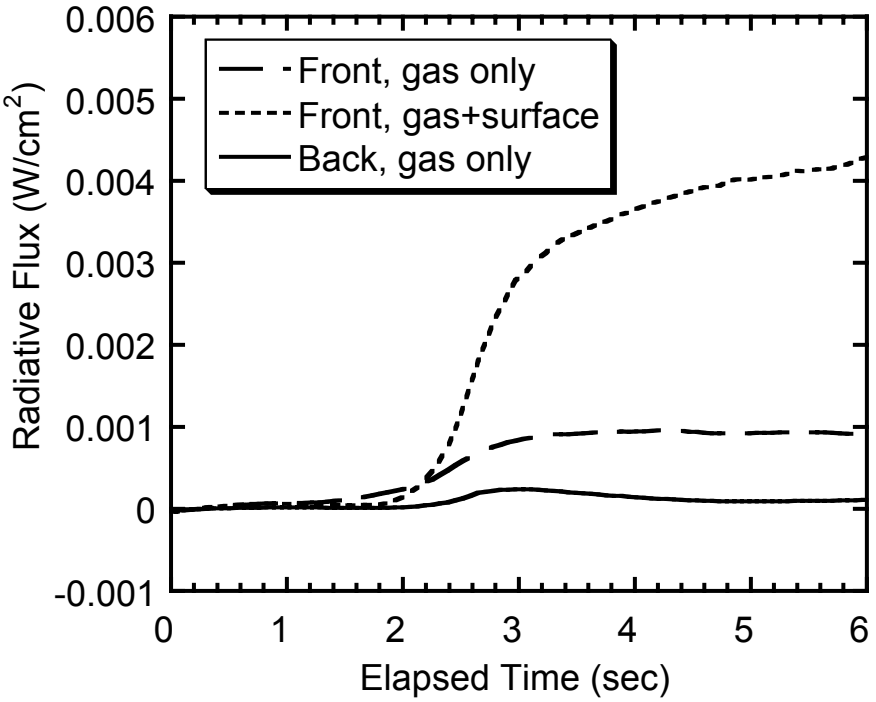

Figure 5. Radiative flux characteristics of flames spreading over polyphenolic foam fuel. See Experimental Apparatus section for discussion of the interpretation of radiometer data.
(b) 40%% O_2 - 60% CO_2, 4 atm, 1g.

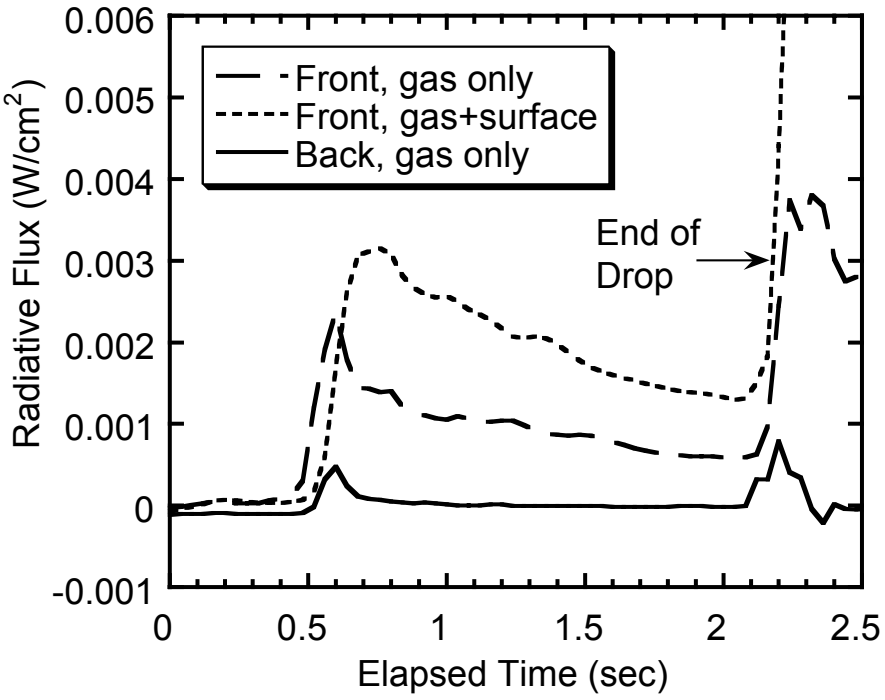

Figure 5. Radiative flux characteristics of flames spreading over polyphenolic foam fuel. See Experimental Apparatus section for discussion of the interpretation of radiometer data.
(c) 40%% O_2 - 60% N_2, 4 atm, μg.

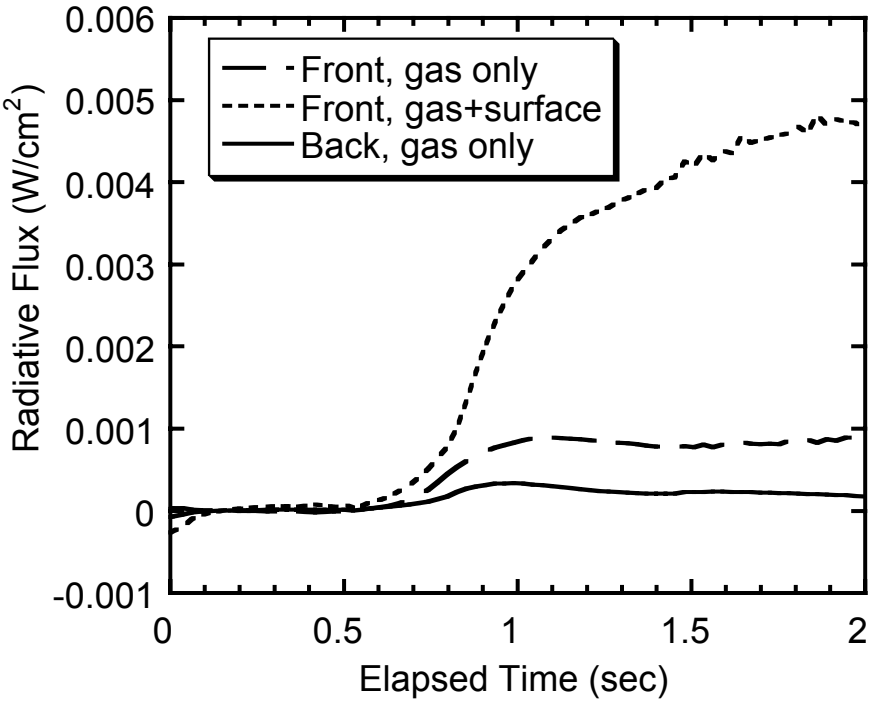

Figure 5. Radiative flux characteristics of flames spreading over polyphenolic foam fuel. See Experimental Apparatus section for discussion of the interpretation of radiometer data.

(d) 40%% O_2 - 60% N_2, 4 atm, 1g.